Cation exchange membrane behaviour of extracellular polymeric substances (EPS) in salt adapted granular sludge

D. Sudmalis [a, *, 1], T.M. Mubita [a, b, 1], M.C. Gagliano [b], E. Dinis [a, b], G. Zeeman [a], H.H.M. Rijnaarts [a], H. Temmink [a]

[a] Department of Environmental Technology, Wageningen University and Research, Bornse Weilanden 9, 6708, WG, Wageningen, the Netherlands
[b] Wetsus, European Centre of Excellence for Sustainable Water Technology, Oostergoweg 9, Leeuwarden, MA, 8911, the Netherlands

ARTICLE INFO

ABSTRACT

This paper aims to elucidate the role of extracellular polymeric substances (EPS) in regulating anion and cation concentrations and toxicity towards microorganisms in anaerobic granular sludges adapted to low (0.22 M of Na^+) and high salinity (0.87 M of Na^+). The ion exchange properties of EPS were studied with a novel approach, where EPS were entangled with an inert binder (PVDF-HFP) to form a membrane and characterized in an electrodialysis cell. With a mixture of NaCl and KCl salts the EPS membrane was shown to act as a cation exchange membrane (CEM) with a current efficiency of ~80%, meaning that EPS do not behave as ideal CEM. Surprisingly, the membrane had selectivity for transport of K^+ compared to Na^+ with a separation factor (S_{K^+/Na^+}) of 1.3. These properties were compared to a layer prepared from a model compound of EPS (alginate) and a commercial CEM. The alginate layer had a similar current efficiency (~80%.), but even higher S_{K^+/Na^+} of 1.9, while the commercial CEM did not show selectivity towards K^+ or Na^+, but exhibited the highest current efficiency of 92%. The selectivity of EPS and alginate towards K^+ transport has interesting potential applications for ion separation from water streams and should be further investigated. The anion repelling and cation binding properties of EPS in hydrated and dehydrated granules were further confirmed with microscopy (SEM-EDX, epifluorescence) and ion chromatography (ICP-OES, IC) techniques. Results of specific methanogenic activity (SMA) tests conducted with 0.22 and 0.87 M Na^+ adapted granular sludges and with various monovalent salts suggested that ions which are preferentially transported by EPS are also more toxic towards methanogenic cells.

1. Introduction

In anaerobic wastewater treatment systems, high monovalent salt concentrations are considered to negatively affect microbial activity, especially of the methanogenic population (Rinzema et al., 1988; Vyrides et al., 2010; Fang et al., 2011; De Vrieze et al., 2016). It was only recently shown that anaerobic granules adapted to approximately 0.35 M Na^+ can increase in size (Gagliano et al., 2017) and can even be formed from dispersed biomass (Sudmalis et al., 2018a) at Na^+ concentrations as high as 0.87 M, while maintaining high methanogenic activity for successful high rate anaerobic reactor operation. This high methanogenic activity could

in part be explained by production of osmolytes by the dominant methanogens allowing to balance the osmotic pressure between the microbial cells and the bulk liquid (Sudmalis et al., 2018b). The toxic effect of highly saline environments on anaerobic microbial consortia has mainly been attributed to cations rather than anions (McCarty and McKinney, 1961; Kugelman and McCarty, 1965; Lin and Chen, 1999; Karri et al., 2006; Lefebvre et al., 2007; Altaş, 2009; Fang et al., 2011) and has been explained by various mechanisms, i.e., their ability to replace metallic enzyme cofactors thereby disrupting the biological function of these cofactors, induction of redox reactions with cellular thiols, provoking Fenton-type reactions that produce reactive oxygen species and by interference with membrane transport processes (Harrison et al., 2007; Chen et al., 2014).

In anaerobic granular sludge, microorganisms are entangled in a matrix of extracellular polymeric substances (EPS) forming a dense spherical biofilm structure (Zhou et al., 2006; Seviour

---

et al., 2012). Extracellular polymeric substances generally have a net negative charge (Liu and Fang, 2003; Ajao et al., 2018), which enables them to adsorb (multivalent) heavy metals (Toner et al., 2005; Comte et al., 2006b; Comte et al., 2008; d'Abzac et al., 2013; Li and Yu, 2014; Dobrowolski et al., 2017). Sorption of monovalent cations by EPS of pure cultures of marine bacteria has also been shown. While the EPS of *Halomonas sp.* were shown to poorly adsorb monovalent cations (Gutierrez et al., 2012), the EPS of *Pseudoalteromonas* have a high affinity towards K^+ sorption (Gutierrez et al., 2008). Due to ability of cation sorption, EPS can alleviate toxicity of low concentrations (mg/L range) of metals towards microorganisms (Teitzel and Parsek, 2003; Harrison et al., 2007; Flemming and Wingender, 2010; Wang et al., 2013) by binding and coordination reactions between the metals and the negatively charged functional groups of EPS, which prevents their diffusion into the deeper parts of the biofilm (Teitzel and Parsek, 2003; Horn and Morgenroth, 2006; Hu et al., 2007). A recent microscopy study of our group has shown that mannose-rich EPS surrounding methanogenic cells in high salinity adapted granular sludge adsorb high concentrations of sodium (Gagliano et al., 2018). These results suggest that even at high salinity EPS may have a protective role against monovalent cations such as Na^+ by hindering their diffusion into microbial cells (Gagliano et al., 2018).

At high concentrations (0.2 M) Cl^- has been reported to cause toxicity to aerobic acidophilic microorganisms because the flux of Cl^- into microbial cells alters the intracellular pH (Suzuki et al., 1999). In general, anions are typically reported to be less toxic for anaerobic microorganisms than cations. However, no attempts to explain this lower toxicity seem to have been reported. In principle, anions and cations both contribute to osmotic pressure in water (Smith et al., 2016), and therefore microorganisms should have a strategy to cope with high concentrations of either of them. Theoretically the negative charge of EPS should prevent or hinder the transport of anions to microbial cells, thereby lowering their toxicity towards the microorganisms present in porous biofilm structures, such as sludge granules. However, this ability of EPS to partially repel anions has not been experimentally demonstrated. Thus far, only few studies focused on the transport rather than sorption of monovalent ions (e.g., K^+, Na^+, Cl^-) in EPS layers. In one study Siegrist and Gujer (1985) experimentally determined the diffusion coefficients of Br^- and Na^+ in a heterogeneous biofilm, and found that these values were smaller compared to their diffusion coefficients in water. Additionally, the diffusion coefficient of Br^- in biofilm was slightly higher compared to Na^+. In another study, Horn and Morgenroth (2006) studied the diffusion of NaCl and $NaNO_3$ in biofilms, but the transport of individual ionic species could not be distinguished because conductivity, rather than individual ion concentrations, was measured.

In the current study, the distribution of monovalent ions (K^+, Na^+ and Cl^-) was investigated in microbial granules adapted to 0.87 M and 0.22 M of Na^+. Initial results indicated that Cl^- is repelled from the granular sludge by EPS surrounding the microorganisms. To verify this, the ion-exchange nature of EPS was investigated. This was done with a novel approach, where EPS extracted from anaerobic granular sludge were used to fabricate EPS layers (EPS-membranes) and these were tested in an electrodialysis cell for transport of K^+, Na^+ and Cl^-. Finally, to study if the ions with the highest transport rate would also more negatively affect methanogenic activity, the effect of different concentrations of Na^+ and K^+ towards specific methanogenic activity (SMA) of 0.87 M and 0.22 M Na^+ adapted granular sludge was determined.

2. Materials and methods

2.1. Source of anaerobic granular sludge

Anaerobic granular sludge was obtained from laboratory scale Upflow Anaerobic Sludge Blanket (UASB) reactors. The reactors were operated at Na^+ concentrations of 0.22 (R5) and 0.87 (R20) M as described in Sudmalis et al. (2018a).

2.2. Ion distribution and concentration within salt adapted granular sludge

2.2.1. Scanning electron microscopy with energy dispersive X-ray spectroscopy (SEM-EDX)

Samples of granules for SEM-EDX analysis were prepared with a modified procedure described in Ismail et al. (2010). The modifications included dehydration with graded series (10, 30, 50, 70 and two times 100%) of ethanol instead of acetone and sputter coating with tungsten instead of platinum. Tungsten was chosen for sputter coating due to its lower grain size compared to platinum, and therefore possibility for imaging at higher magnifications (Bell et al., 1987; Echlin, 2009). The granules were imaged at an acceleration voltage of 10 kV and a beam current of 0.4 nA, at room temperature in a field emission scanning electron microscope (Magellan 400, FEI Company, Oregon, USA) equipped with energy dispersive X-ray detector. The images were processed using AZtec software (OXFORD Instruments).

2.2.2. Ion concentration in hydrated granular sludge

Approximately 20 g of sludge samples for determination of ion concentrations in hydrated granular sludge were taken directly from R5 and R20 through a sampling port located 7.5 cm from the bottom of the reactor columns with a total column height of 65 cm. For ionic composition measurements of hydrated granular sludge, the sludge was first separated from the liquid phase by centrifugation at 10000 xg and 4 °C for 15 min. Further, the sludge samples were carefully homogenised with a spatula and two samples (approximately 0.5 g each) of homogenised solids were taken for microwave digestion (ETHOS 1 - Advanced Microwave Digestion Labstation, Milestone S.r.l., Italy) with 10 mL of 65% HNO_3 (For Analysis Emsure® ISO). Digested samples were brought up to 50 mL with mili-Q water and further diluted for analysis. As a blank for ionic composition of solids mili-Q was treated in the same way as the samples. The supernatant after centrifugation was filtered through 0.2 μm cellulose acetate membrane filter (VWR® Syringe Filters) and diluted with mili-Q for further analysis. The filtered supernatant from this point forward will be referred to as the bulk liquid throughout the manuscript. Measurements of bulk liquid were made in one replicate to confirm the expected bulk liquid concentrations of ions. Differences between measurements and expected values were below 2% in all cases.

Additionally, to elucidate the cation exchange properties of EPS in sludge granules, the distribution of Cl^-, Na^+, and K^+ in granules of R20 upon granular sludge exposure to equimolar K^+ (0.87 M) concentration was investigated. To do this, 1 g of R20 granular sludge was immersed in 1L of a modified ($NaHCO_3$ and NaCl replaced with $KHCO_3$ and KCl, respectively) nutrient medium of R20 (Sudmalis et al., 2018a) for 24 h before analysis of ionic composition with sample preparation as described above. A period of 24 h for ion exchange was chosen to ensure that an equilibrium between the sludge granules and the modified nutrient medium is reached. As a control R20 granular sludge was also exposed to its original medium containing 0.87 M of Na^+ (Sudmalis et al., 2018a).

Analysis of Na^+ and K^+ was carried out by inductively coupled plasma optical emission spectroscopy (ICP-OES, Varian, Australia)

as described in Gagliano et al. (2018). Chloride content was measured on Dionex ICS-2100 Ion Chromatography System (Breda, The Netherlands) equipped with a Dionex IonPac AS19 column (4 × 250 mm) and data were processed with Chromeleon 6.80 SR13 software. The results are presented on weight bases ($mmol_{ion}/g_{medium}$ and $mmol_{ion}/g_{wet\ sludge}$) to prevent introduction of errors due to differences in the density of the medium and the granular sludge.

2.3. Ion exchange properties of EPS

2.3.1. Extraction and purification of EPS

Extracellular polymeric substances (EPS) were extracted from granular sludge adapted to 0.87 M of Na^+ (R20) by using an alkaline extraction method as reported by Felz et al. (2016). In short, 3 g of granular sludge (wet weight) were put into a 0.5% (w/v) Na_2CO_3 solution, heated to 80 °C and stirred at 400 rpm for 35 min. After extraction, the cell debris and insoluble fraction of the extract were separated by centrifugation at 4000 xg and 4 °C for 20 min. Finally, the EPS solution was dialysed (SnakeSkin™, 3.5K MWCO) against milli-Q for 24 h. To obtain purified EPS in a dry state, the EPS solution was further lyophilised at −84 °C and 0.001 mbar.

2.3.2. Fabrication of alginate gel layers (ALG − membranes)

Extracellular polymeric substances are a mixture of proteins, polysaccharides, nucleic acids, amyloids, lipids and glycoproteins with proteins and polysaccharides often being the main constituents of EPS (Seviour et al., 2019). Amongst all of these constituents, alginate and alginate-alike molecules (anionic polysaccharides) are frequently reported to be found in pure cultures of microbial cells as well as in microbial aggregates (Körstgens et al., 2001; Lin et al., 2009, 2010; Flemming and Wingender, 2010). Therefore, alginate layers were prepared as a control for comparison of their ion exchange properties with layers prepared by using the EPS extracted from granular sludge. The alginate gel layers (ALG-membranes) were casted with an external gelation method adapted from Li et al. (2015) in following steps: i) dissolving the polymer in 10 mL milli-Q; ii) degassing the solution for 24 h at 4 °C; iii) casting the solution on a petri dish (ID = 5.7 cm) and drying at 40 °C in a levelled oven; iv) crosslinking the casted layers in a 2% (w/v) calcium chloride solution with 30% (v/v) of ethanol. For casting a mixture of 0.4 g of sodium alginate (SA) and 0.004 g of guar gum (GG) as a plasticiser were used, resulting in 0.016 g SA/cm^2. The resulting membrane was washed with demi-water and equilibrated in a solution with 10 mM NaCl and 10 mM KCl for 8 h before ion selectivity tests.

2.3.3. Fabrication of layers with EPS (EPS-membranes)

First, a polymeric solution was prepared by dissolving poly(-vinylidene fluoride-co-hexafluoropropene) (PVDF-HFP) in dimethyl acetamide (DMAc) in a ratio 1:9.5 w/v for 3 h at 80 °C. Then, a weighed amount of EPS was dispersed in the polymeric solution and the materials were blended in a ball mill for 4 h. The resulting mixture contained 70:30 wt ratio of PVDF-HFP to EPS. The mixture was cast onto a glass plate at 50 °C until complete evaporation of the solvent. The resulting layer (EPS-membrane) was washed with demi-water and equilibrated in a solution with 10 mM NaCl and 10 mM KCl for 8 h before ion selectivity tests. The content of EPS in the EPS-membrane was approximately 0.0027 g EPS/cm^2 of dry membrane. This was calculated from the total area of the membrane by assuming a uniform EPS distribution.

2.3.4. Confocal laser scanning microscopy (CLSM) for visualisation of EPS distribution in the polymeric binder PVDF-HFP

To visualize the EPS distribution in the EPS-membranes, the membranes were first equilibrated in a buffer solution (10 mM KCl and 10 mM NaCl) overnight. For the staining of the protein fraction of EPS, the EPS-membranes were placed in PBS 1X and SYPRO Ruby (Invitrogen Molecular Probes, USA) for 1 h in the dark. Finally, the membranes were washed with the buffer solution and immediately observed under CLSM. To guarantee that SYPRO Ruby does not stain PVDF-HFP, a pure PVDF-HFP membrane was processed in the same way as EPS-membranes. Before the CLSM analysis, auto-fluorescence of PVDF-HFP was tested, as described in Appendix 1. Microscopy analysis was performed with an inverted AxioObserver Zeiss LSM 880 CLSM (Carl Zeiss, Germany) with a 40 × /1.3 Oil DIC M27 Plan-Apochromat objective lens. Autofluorescence of PVDF-HFP in the membranes was visualised with 488 nm excitation wavelength, at a maximum emission of 510 nm. SYPRO Ruby signal was visualised with 458 nm excitation wavelength at a maximum emission of 656 nm. The argon laser was set to 1% power for both excitation wavelengths. A series of Z-axis images (212.5 μm × 212.5 μm x 70 μm) were generated by optical sectioning with a slice thickness of 1 μm. Maximum projection intensity and orthogonal 3D reconstruction were generated with Zen Blue software (Zen imaging Software, ZEISS, Germany). The choice of emission wavelengths and the dye for EPS protein staining is explained in detail in Appendix 1.

2.3.5. Electrochemical characterization and ion selectivity

Performance of the layers as ion exchange membranes was evaluated in a six-compartment electrodialysis cell as shown in Fig. 1. Different membranes separated the compartments inside the cell: i) the membrane under investigation, placed in between compartments A and B. This membrane was either EPS-membrane, ALG-membrane or a commercial membrane (Neosepta CMX, ASTOM Corporation, Tokyo, Japan) used as a comparison. ii) Commercial ion exchange membranes, i.e., Neosepta AMX and CMX, which separated the other compartments. Characterization of the membranes was done with a solution containing a mixture of two different monovalent cations, i.e., K^+ and Na^+ as chloride salts, allowing for direct comparison of monovalent ion transport through the membranes in multi-ion solutions. Before each experiment, all membranes were equilibrated in a mixed cation solution (10 mM NaCl + 10 mM KCl) for 8 h, which allows any weakly adsorbed ion to diffuse to the bulk solution and the exchange of some Na^+ for K^+.

Compartments A, B, and C were filled with a solution containing 10 mM NaCl and 10 mM KCl, whereas compartments D were filled with 0.1 M Na_2SO_4 solution. Compartments A and B were filled with 130 mL solutions that were continuously stirred. For compartments C and D, 1L solutions were circulated at a flow rate of 170 mL/min to keep the ion concentrations constant throughout the experiment. A current density of 10 A/m^2 was applied to the cell for 1 h. Samples from compartments A and B were taken over time and ion concentration was measured by ion chromatography. An increase in chloride concentration was calculated from compartment A, whereas increases in sodium and potassium concentration were calculated from compartment B. Ion selectivity (S) in the membranes is based on the concentration changes between potassium and sodium and is given by

$$S_{K^+/Na^+} = \frac{\Delta c_{K^+}}{\Delta c_{Na^+}}, \qquad \text{Eq. 1}$$

and

$$\Delta c = c_t - c_{initial}, \qquad \text{Eq. 2}$$

where t, $c_{initial}$ and c_t are the sampling time, the initial concentration and the concentration at time t measured in compartment B,
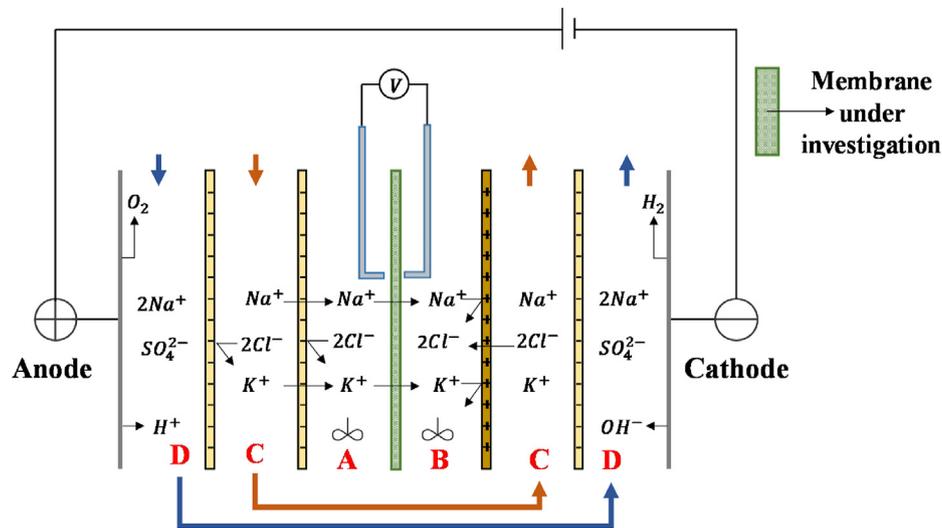
Fig. 1. Schematic representation of the electrochemical cell used to evaluate the performance of the membranes. The membrane under investigation separates compartments A and B. After applying a potential difference, cations move from compartment A to B. For an ideal cation-exchange membrane, the transport of chloride from compartment B to A is zero. Water splitting was not relevant in these experiments.

respectively.

The ability of the membrane to allow the transport of only one type of ion (cations or anions), the permselectivity, was characterized as current efficiency (η)

$$\eta = \sum_{i}^{i=2} \frac{(c_{t,i} - c_{initial,i}) \cdot V_{cell} \cdot F}{I \cdot t} \qquad \text{Eq. 3}$$

where subscript i refers to cation species in solution, i.e., potassium and sodium, V_{cell} is the volume of liquid in compartment B (L), F is Faraday's constant (96485 C/mol), I is the applied current (A) and t is time (s).

The current efficiency gives an indication on how selectively ions are transported across the membrane (Sadrzadeh and Mohammadi, 2009), i.e., it indicates if the ionic current is mainly transported by potassium and sodium (cation-exchange membrane), or the membranes also allow the transport of chloride.

2.4. Effect of anions and cations on specific methanogenic activity

To study the effect of monovalent anions and cations on specific methanogenic activity (SMA) of salt adapted granular sludge, batch experiments in 118 mL serum bottles at a working volume of 50 mL, 120 RPM mixing speed and 35 °C were performed. The VSS concentration was set to 1 g/L and the COD:VSS ratio was 4:1 (w/w). Sodium acetate was used as the electron donor and carbon source. The SMA was calculated through measurements of pressure build-up curves with a pressure meter equipped with an absolute pressure probe (GMH3151, Greisinger Electronic, Germany). The biogas composition at the end of experiments was measured as described in Steinbusch et al. (2008). Unless stated otherwise, the experiments were performed in triplicate. All results were corrected for the atmospheric pressure and pressure build-up in blank experiments without added acetate.

The first set of experiments was performed to study the SMA of granular sludge adapted to 0.22 (R5) and 0.87 (R20) M of Na^+, when exposed to equimolar concentration of cations by addition of NaBr, KCl and KBr. The second set of experiments was performed to study the SMA of R5 granular sludge upon exposure to hyper-salinity shocks (i.e., an abrupt increase of salinity by spiking a nutrient

medium with increased ion concentration) of NaCl, NaBr, KCl and KBr. The final cation concentration in these experiments was 0.43 M. Bromide salts were tested (NaBr and KBr), to investigate if different anions at very high salinity would also have a substantial effect on SMA, as is frequently reported for cations (Kugelman and McCarty, 1965; Lefebvre et al., 2007; Fang et al., 2011). All experiments contained 0.08 M of Na^+ originating from inocula and sodium acetate as a carbon source. This was taken into account when calculating the desired concentration of cations in the experiments. The nutrient medium was the same as reported earlier (Sudmalis et al., 2018b). NaCl, NaBr, KCl and KBr salt amounts were calculated to reach the desired cation concentration for each experiment.

3. Results

3.1. Equilibrium of sodium, chloride and potassium in granules at different salinities

The measured ion concentrations (Fig. 2) and distributions (Fig. 4) in the anaerobic, salt adapted, granular sludges show high affinity of EPS towards cations compared to anions. Fig. 2-A, B show the Na^+ and Cl^- concentrations in the bulk liquid and in granular sludges of R5 and R20, respectively. Sodium concentration in the granular sludge was 0.24 ± 0.004 (~0.24 M) and 0.71 ± 0.01 (~0.71 M) mmol/$g_{wet\ sludge}$ in R5 and R20, respectively. The Na^+ concentration in R5 granular sludge was 9% higher compared to the bulk liquid, whereas in R20 it was 17% lower compared to the bulk liquid. The Cl^- concentration was 0.11 ± 0.002 (~0.11 M) and 0.52 ± 0.001 (~0.52 M) mmol/$g_{wet\ sludge}$ in R5 and R20, respectively (Fig. 2-A, B). These concentrations correspond to a 31.2 and 35.8% lower Cl^- concentration compared to the bulk liquid in R5 and R20, respectively. Thus, apparently EPS of granular sludge acclimated to 0.22 and 0.87 M of Na^+ preferentially repel anions, such as Cl^-, probably due to anionic nature of EPS, as will be discussed in more detail in Section 4.1.

Potassium concentration in the R20 granular sludge before changing the medium was 0.05 mmol/$g_{wet\ sludge}$ (~0.02 g/$g_{sludge\ VS}$) (Fig. 3). This corresponds to a 28 fold increase compared to the growth medium. Such a high concentration of K^+ can be found within methanogenic cells upon exposure to high osmotic stress,
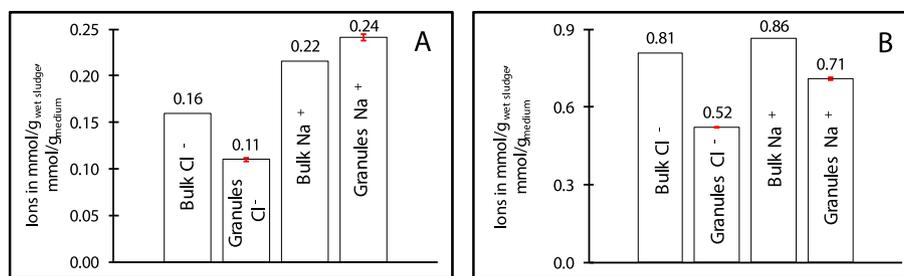
Fig. 2. Na$^+$ and Cl$^-$ concentration in salt adapted granular sludge. A − granular sludge and bulk liquid composition of R5 adapted to 0.22 M Na$^+$; B - granular sludge and bulk liquid composition of R20 adapted to 0.87 M Na$^+$. The error bars show absolute deviation from measurements of two separately prepared and digested 0.5 g sludge samples.
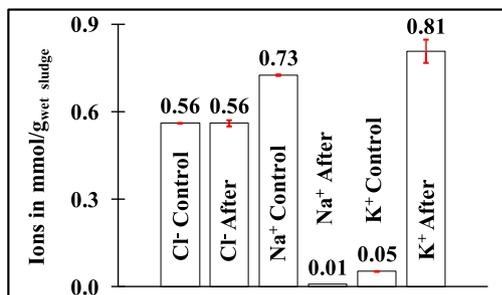
Fig. 3. Ionic composition of R20 granular sludge after 24 h in 0.87 M Na$^+$ medium (control) and 0.87 M K$^+$ medium (after). The error bars show absolute deviation from duplicate measurements.

even after accumulation of osmolytes within the microbial cells (Sowers and Gunsalus, 1995). When placing the R20 granules, previously exposed to 0.87 M Na$^+$, in a nutrient medium with K$^+$ (0.87 M), the Cl$^-$ concentration in the granular sludge did not change (Fig. 3). However, Na$^+$ had almost completely been displaced with K$^+$ within 24 h (Fig. 3). This indicates a cation exchange nature of EPS in the anaerobic granular sludge. After the medium change, the K$^+$ concentration within the granular sludge reached a concentration of 0.81 ± 0.04 mmol/g$_{wet\ sludge}$ (~0.32 g/g$_{sludge\ VS}$), which is higher compared to the Na$^+$ concentration of 0.73 ± 0.002 mmol/g$_{wet\ sludge}$ in the control sample. This shows a higher EPS sorption capacity of K$^+$ in granular sludge compared to Na$^+$ at a given molarity.

Scanning electron microscopy with energy dispersive X-ray spectroscopy (SEM-EDX) of sliced microbial granules adapted to 0.87 M of Na$^+$ showed a uniform distribution of Na$^+$ ions throughout the granules (Fig. 4-A), confirming the ionic composition results in Fig. 2. In contrast to the ion chromatography results (Fig. 2), Cl$^-$ could not be detected in the granules with SEM-EDX imaging (Fig. 4-B). This could be a result of Cl$^-$ ions removal together with water from the pores of the granular sludge during the dehydration steps of the SEM samples preparation (see Materials and methods). This removal of Cl$^-$, coupled with Na$^+$ retention in the granules, suggests that Na$^+$ was bound to the EPS, whereas chloride was mainly present in the water phase of the granule pores as will be further discussed in Section 4.2.

The binding of Na$^+$ to EPS was further verified via fluorescent CoroNa Red Na$^+$ staining on R5 and R20 hydrated granules (Appendix 4). Microscopy analysis confirmed the presence of Na$^+$ in the EPS matrix surrounding granules (Fig. S4), while the quantification of the CoroNa red signal emission of R5 and R20 granules' cells (Appendix 4) showed that the average intracellular Na$^+$ concentration was in the range 55−66 mM in both granules. These results confirmed the binding properties of such EPS towards Na$^+$.

3.2. The ion exchange properties of EPS-membrane and ALG-membrane

The CLSM analysis showed that binding of EPS with PVDF-HFP was successful (Fig. 5-A, C), with a uniform distribution of EPS (in red, stained with Sypro RUBY) as a thin layer on the surface of the PVDF-HFP (in green). Such a distribution is likely due to the hydrophobic nature of PVDF-HFP, which could only interact with the hydrophobic moieties of otherwise largely hydrophilic EPS, and did not allow for penetration of EPS in the depth of the membrane. The negative control staining (Fig. 5-B, D) confirmed that SYPRO Ruby does not bind to PVDF-HFP membranes and that the signal in Fig. 5-
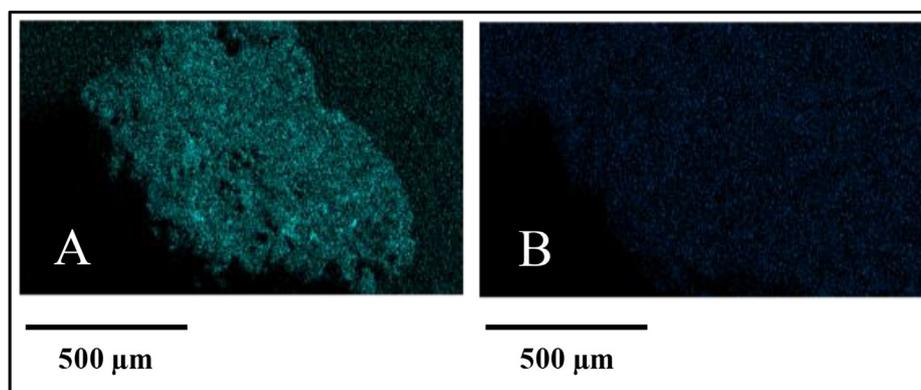
Fig. 4. SEM − EDX micrographs of a sliced microbial granule adapted to 0.87 M Na$^+$. A − distribution of Na$^+$ throughout the granular structure. B − distribution of Cl$^-$ throughout the granular structure. The black corner in the bottom left of the micrographs is a region from which the detector could not receive any signal due to the structure of the granule. No clear shape of a granule in B indicates that the background signal was as strong as the signal from the granule.
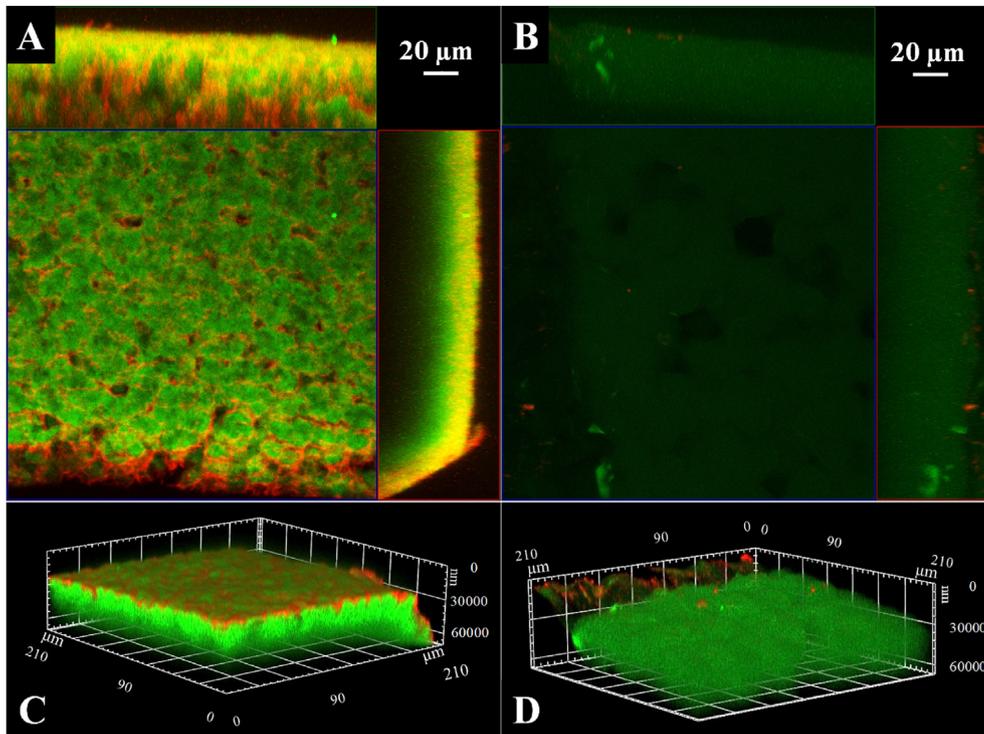
Fig. 5. A, B - Orthogonal view of CLSM Z-stack images of membranes after Sypro RUBY staining and the respective 3D reconstructions in C, D. The membrane with the EPS in A, C. The reference membrane composed solely of PVDF-HFP in B, D. The green signal shows auto-fluorescence of PVDF-HFP. The red signal shows EPS proteins stained with SYPRO Ruby. The bright yellow signal originates from the combination of green and red. (For interpretation of the references to colour in this figure legend, the reader is referred to the Web version of this article.)

A, C indeed originated from Sypro Ruby bound to proteinaceous fraction of EPS.

After successful preparation of the membranes as shown in Fig. 5-A, C, their selectivity towards transport of K^+, Na^+ and Cl^- was tested in an electrodialysis cell. Fig. 6-I, II, and III show changes in K^+ and Na^+ concentration in compartment B and of Cl^- concentration in compartment A, for the ALG-membrane, EPS-membrane, and the commercial membrane, respectively. Cations were preferentially transported across the membranes, whereas Cl^- ions were partially repelled. In addition, a preferential transport of K^+ over Na^+ across the ALG and EPS-membrane was measured (Fig. 6-I, II). The rate of change in ion concentration (determined by the slopes of the curves, m value) shows that in the ALG-membrane the K^+ transport was 11% higher and Na^+ transport was 23% lower than in the EPS-membrane. The resulting potassium selectivity ($S_{K^+/Na^+} > 1$) is depicted in Fig. 6-IV and was higher for the ALG-membrane compared to EPS-membrane. With the commercial ion exchange membrane, there was no markedly difference in the transport between K^+ and Na^+ (Fig. 6-III, IV). In Fig. 6-IV, the current efficiency shows how much of the current was transported by cations. Despite the non-ideal cation selectivity of the "bio-membranes", the current efficiency was relatively high: 79% for the ALG-membrane and 83% for the EPS-membrane. The commercial membrane gave the highest current efficiency of 92%.

3.3. Effect of anions and cations on specific methanogenic activity

Fig. 7–A shows that exposure of 0.22 M Na^+ adapted granular sludge to equimolar concentration of KCl and KBr salts resulted in a decrease of methanogenic activity by 25.3 and 11.7%, respectively, when compared to the reference at 0.22 M of Na^+. Doubling the ion concentration to 0.43 M of KCl and KBr resulted in SMA decrease by

49.2 and 44.1%, respectively. The negative effect of Na^+ salts on the SMA of granular sludge at increased molarity of 0.43 M was considerably less pronounced compared to K^+ salts (Fig. 7–A). The SMA decreased by 19.9 and 11.1% with NaCl and NaBr salts, respectively. It seems that in general Br^- salts had a slightly smaller negative effect on SMA compared to Cl^- salts (Fig. 7-A). However, the results obtained with NaBr at 0.22 M (Fig. 7-A) did not follow the overall trend, therefore additional experiments are needed in the future to confirm this.

Finally, the 0.87 M Na^+ adapted granular sludge could retain its methanogenic activity when exposed to equimolar concentration of NaBr (Fig. 7-B). NaBr had no clear negative effect on the SMA, whereas 0.87 M of K^+ salts resulted in complete loss of methanogenic activity. Overall, the results of the SMA tests clearly show that at equimolar concentrations of monovalent salts, the methanogenic activity of salt (NaCl) adapted granular sludge was more influenced by changing the cations (Na^+ to K^+) than by changing the anions (Cl^- to Br^-).

4. Discussion

4.1. Cation exchange membrane properties of EPS and potassium selectivity

In one of our previous studies mannose-rich EPS of anaerobic granular sludge adapted to high salinity was shown to bind Na^+ (Gagliano et al., 2018). The current results further demonstrate that the EPS matrix of granules grown at 0.22 (R5) and 0.87 M of Na^+ (R20) is indeed able to retain high Na^+ concentrations (Figs. 2 and 4 and Fig. S4). Even though the sodium concentration in granules of R20 was lower compared to the bulk liquid (Fig. 2), it is worth noticing that the granules in R5 contained considerably less Na^+

(approx. 3 times) compared to R20 granules. Sorption behaviour of EPS can be characterized by Freundlich and/or Langmuir sorption isotherms as reported by Dobrowolski et al. (2017). Thus, such differences can be explained by the fact that in R20 potentially the maximum EPS Na^+ sorption capacity was reached, while it was not the case in R5 granules. It is also not excluded, that these maximum sorption capacities differ in R5 and R20, because it is known that, as a response to a high salinity, the chemical composition of EPS in anaerobic sludges changes in time (Vyrides and Stuckey, 2009). In fact, we have recently shown that the EPS glycoconjugate composition of granules grown under the same conditions as R5 is different compared to those grown under conditions as in R20 (Gagliano et al., 2018). It is not clear whether the Na^+ sorption capacity of R5 and R20 granules was similar from the start. However, experiments in continuously operated UASB reactors, where the influent of R5 was exchanged with R20 for a period of two weeks, showed that the new ion equilibria became very similar i.e., Na^+ and Cl^- concentration in R5 granules became very comparable to R20 granules and vice versa (Appendix 5). This is an interesting result, because it shows that anaerobic granules grown under very different salt conditions reach very similar cation and anion equilibria upon exposure to new environmental conditions.

When these EPS were extracted from R20 granules and entangled in a layer with an inert binder (PVDF-HFP), these layers behaved as cation exchange membranes (CEM), i.e., partially repelled anions, such as Cl^- and selectively transported cations, such as K^+ and Na^+ (Fig. 6-I, II). This is probably the result of the abundant presence of different negatively charged functional groups such as carboxylic, phenolic and phosphoric groups in EPS (d'Abzac et al., 2013). The same CEM ability was shown also for the ALG-membranes, most likely because of abundance of negatively charged carbonyl groups at neutral pH in alginate (Nestle and Kimmich, 1996; Lee and Mooney, 2012).

The EPS and ALG-membranes were not fully cation selective (Fig. 6) since the transport of cations (Na^+ and K^+) represented ~ 80% of the total ionic current (Fig. 6-IV). Thus, 20% of the ionic current can be attributed to transport of Cl^-. Such non-ideal cation exchange nature of EPS would be desirable from a microbial perspective, because ideal behaviour would prevent diffusion of important substrates, such as phosphate or acetate, to the microbial cells. From a physical-chemical perspective some transport of anions, such as Cl^-, through EPS-membranes and alginate-membranes is expected due to their hydrogel nature. Hydrogels are known for their hydrophilic structure, and hence high sensitivity to water: high water uptake, leading to swelling or even dissolution (Lee and Mooney, 2012; Ahmed, 2015). The swelling in the membranes can create non-selective paths/channels for ion (K^+, Na^+, and Cl^-) passage. This is due to decrease of charge density caused by swelling in a membrane with a fixed amount of charges. Such decreased charge density may lead to decreased ion-functional group interactions. Optical coherence tomography (OCT) analysis (Appendix 2) showed that a hydrated PVDF-HFP membrane was 50 μm thick, while addition of 10% w/w EPS increased the membrane thickness by 89 μm, clearly showing that swelling of EPS indeed took place.

Surprisingly, the EPS and particularly the ALG-membrane were more selective to K^+ than to Na^+ (Fig. 6-IV). Such selectivity was not measured in the commercial membrane (Fig. 6-IV) and is known to be difficult to achieve with commercial membranes in general (Luo et al., 2018). It is not clear which EPS and alginate properties resulted in such a selectivity. The low transport of Na^+ compared to K^+ across the membranes may be related to several factors such as i) steric effects due to the higher hydrated size of Na^+ (3.58 Å) than K^+ (3.31 Å) (Nightingale, 1959); ii) strong interactions (e.g., adsorption) between Na^+ and the functional groups in the

membranes (Mubita et al., 2020) and iii) the initial Na:K ratio in the membranes. These factors certainly should be further looked into. It should also be noted, that while the overall cation exchange properties of EPS (repulsion of anions and transport of cations) were unlikely to be significantly altered due to the harsh alkaline extraction method used in this study (comparison of e.g., Figs. 2 and 6), it is known that different extraction methods can result in, e.g., different metal binding ability (capacity) of heavy metals (Comte et al., 2006a; d'Abzac et al., 2010). Thus, in future studies the EPS membranes should be prepared with EPS extracted with various extraction methods, because transport properties of individual cations may also be potentially affected depending on the extraction procedure used.

The current efficiency of ALG-membrane was very similar to that of the EPS-membrane (Fig. 6-IV). Measurements of charge density show a markedly difference between alginate and EPS (Appendix 3). In principle, membranes with high charge density favour the conductivity of counter-ions (Geise et al., 2013). Alginate had a charge density of 7.0 meq/g and EPS a charge density of 2.5 meq/g as measured for free dissolved polymers in solution. These values may be significantly different in the membranes themselves due to charge shielding. In ALG-membranes, the crosslinking with calcium ions may have led to a reduction of charged functional groups available for ion-exchange. In the EPS-membranes, some functional groups may have been completely embedded in the matrix of the supporting polymers (PDVF-HFP). Therefore, in future studies the real charge densities in the membranes themselves should be assessed, for example by acid-base titration (Hosseini et al., 2012).

4.2. Methanogenic activity inhibition by various ions

The methanogenic activity of 0.87 M Na^+ adapted granular sludge was completely inhibited when this sludge was exposed to equimolar concentrations of K^+ (Fig. 7- B). Also, exposure of 0.22 M Na^+ adapted granular sludge to 0.22 M of K^+ led to a 25% decrease in methanogenic activity. The decrease of SMA was smaller (19.9%) when exposing the same granular sludge to 0.43 M Na^+ (Fig. 7-A). Kugelman and McCarty (1965) showed that K^+ had a stronger negative effect on methanogenic activity than Na^+, using low salinity adapted sludge and equimolar concentrations of sodium and potassium bicarbonate. Our results extend this finding with Cl^- salts and high salinity adapted sludge and demonstrate that anions at equimolar concentrations have little influence on the SMA (Fig. 7). The mechanism of a potential Br^- or Cl^- toxicity on methanogens is not known. Possibly anion toxicity is "masked" by the ability of EPS to repel these anions, as was shown in this study (Figs. 2, Figure 3, Fig. 6). This "masking" would occur if granular structure could be viewed upon as a cation exchange membrane (Fig. 8).Appendix 3 The concentration of ions in membranes is determined by the concentration of fixed charged functional groups in it and meets the requirement of electroneutrality according to the following equation (Galama et al., 2013):

$$c_{counter-ion} - c_{co-ion} - X = 0 \qquad \text{Eq. 4}$$

Where $c_{counter-ion}$ is the concentration of the ion with the charge opposite to the functional groups of the membrane (cations in the case of EPS), c_{co-ion} is the concentration of ions with the same charge as the functional groups of a membrane (anions in the case of EPS), and X is the concentration of charged functional groups (negative for EPS). Due to the fixed negative charges of EPS with a concentration X, the concentration of negatively charged co-ions in the porous granular structure can potentially be reduced, while positively charged counterions are allowed to accumulate (Fig. 8).
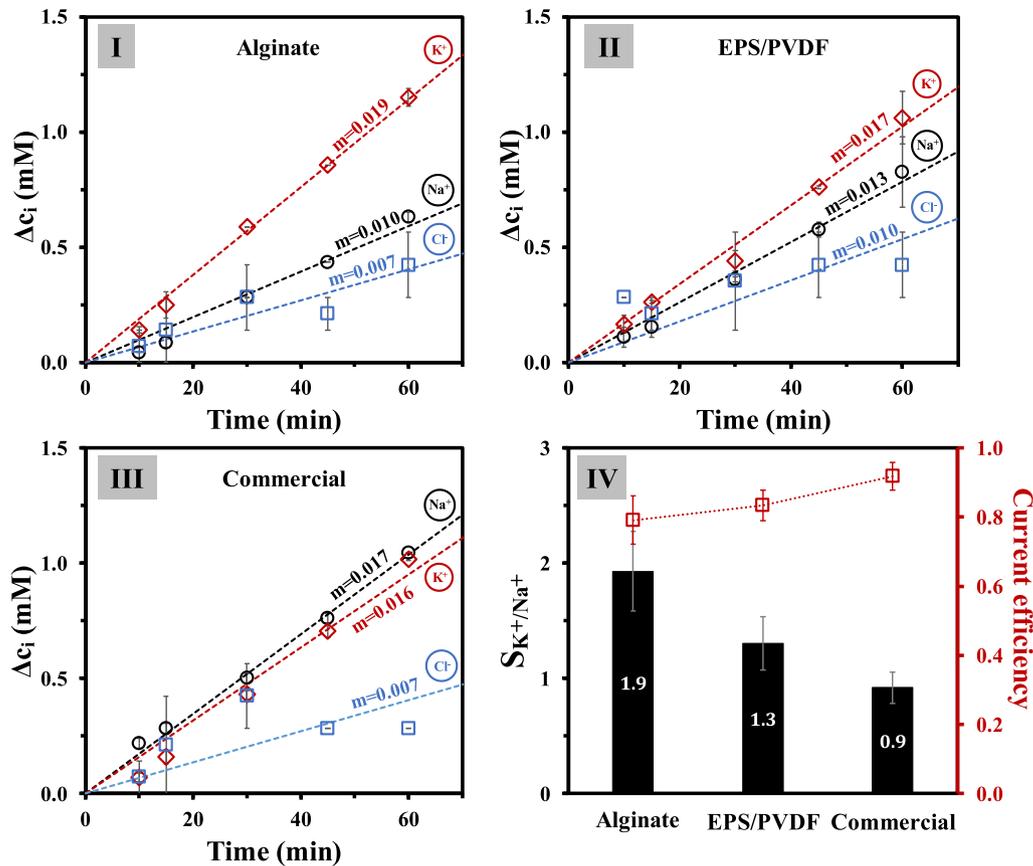
Fig. 6. I, II, III - Ion concentration changes (symbols) as a function of time. The concentration changes of cations are measured in compartment B, whereas the concentration changes of anions was measured in compartment A. The m value indicates the slope of the dashed lines. IV - Potassium selectivity (S_{K^+/Na^+}) and current efficiency of the membranes. The error bars show absolute deviation in duplicate measurements.
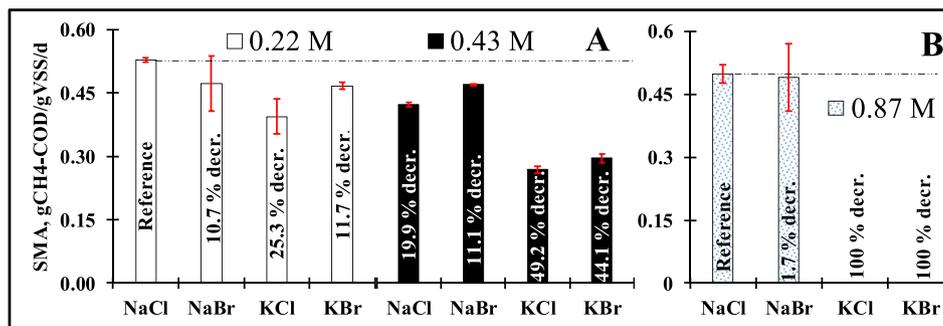
Fig. 7. SMA of granular sludge exposed to various Cl^- and Br^- salts. A − 0.22 M Na^+ adapted granular sludge exposed to equimolar concentration and double concentration of NaCl, NaBr, KCl and KBr; B − 0.87 M Na^+ adapted granular sludge exposed to equimolar concentration of NaBr, KCl and KBr. In B and in experiments with chloride salts in A, the error bars show standard deviations from triplicate experiments. Error bars with Br salts in A show absolute deviations from average in duplicate experiments. % decr. - % SMA decrease with respect to the reference. Horizontal dashed lines show the SMA of the reference.

The extent to which the amount of co-ions is reduced in the granular structure compared to the bulk liquid depends on X. Due to the fixation of the charged functional groups in EPS and their interaction with cations, the osmotic pressure experienced by the microbial cells can be reduced. This was partially proven in this study by evaluating the Na^+ content of methanogenic cells after fluorescent staining (Appendix 4), which was much lower than the surrounding medium (66 mM intracellular versus 0.87 M extracellularly).

This hypothesis can potentially be further tested with EPS deficient mutants of methanogens in toxicity experiments, and by comparing their sensitivity to different anions with EPS covered methanogens. Such an approach has been used by Wang et al. (2013) to study the role of EPS in osmo-protection upon exposure of *Klebsiella pneumoniae* to 100 mM of $CaCl_2$. This showed that in EPS deficient microbial cells the turgor pressure decreased upon exposure to salt, whereas in cells covered with EPS the turgor pressure remained unaffected. This suggests that EPS helps to counteract the osmotic pressure experienced by microbial cells in high salinity environments.
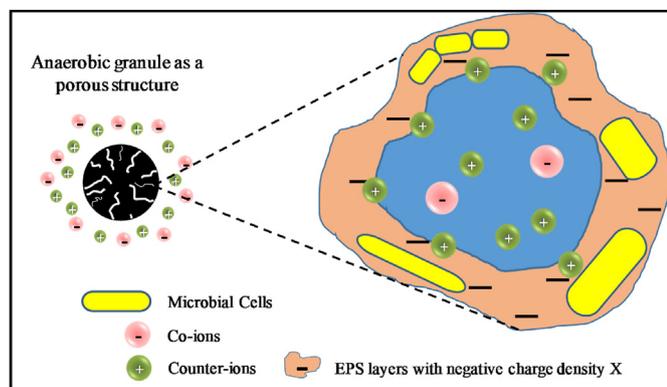
Fig. 8. Graphic representation of granular sludge as a porous structure, with fixed negative charges in EPS that are able to bind positive counter ions.

The mechanism by which high K^+ concentrations inhibit methanogenic activity is not exactly known. Toxicity studies with high concentrations of metallic cations and other types of microorganisms demonstrated interference with membrane transport processes, either by competitively inhibiting membrane transporter proteins or by affecting the membrane potential (Harrison et al., 2007). Acetoclastic methanogens couple Na^+ transport across the cytoplasmic membrane with the transfer of the methyl group from tetrahydrosarcinapterin (H_4SPT) to coenzyme M (HS-CoM). This precedes the final reduction step for methane production from acetate (Welte and Deppenmeier, 2014). Also, acetoclastic methanogens make use of both proton and Na^+ gradients across the cell membrane for ATP synthesis (Welte and Deppenmeier, 2014). Abrupt exposure of the microorganisms to high concentrations of K^+ could potentially interfere with these processes. Prolonged periods (more than a month) of exposure can result in adaptation of methanogens to K^+ concentrations of up to 0.19 M (Chen and Cheng, 2007). However, further increases of K^+ concentration in completely stirred continuously operated tank reactor resulted in decreasing methanogenic activity, similar to results of batch experiments in this study (Chen and Cheng, 2007). This suggests that adaptation of methanogens to high K^+ concentration is more difficult than adaptation to Na^+. Albeit the lower Na^+ toxicity compared to K^+ may be related to decreased ability of EPS to bind K^+ as shown in this study, such direct interpretation should still be performed with care. Firstly, as discussed in *Section 4.1*, the EPS properties to transport or bind cations may change as a result of the extraction method applied. Secondly, the ion selectivity can be different for sorption compared to transport (Epsztein et al., 2019). In principle, this means that the higher K^+ over Na^+ sorption capacity of granules shown in Fig. 3 should not be directly translated to ion transport properties of unextracted EPS. Thirdly, microbial cell membranes contain a high ubiquity of ion transporters (Martin et al., 1999), and these are expected to also play an important role in regulating the ion exchange between the surrounding environment and the cytoplasm of microbial cells. Finally, microbial cells can accumulate compatible solutes to balance osmotic pressure between the cells and the surrounding environment (Martin et al., 2000; Roberts, 2005; Sudmalis et al., 2018b). Thus, the EPS as shown in Fig. 8 can only be viewed as one out of several protective mechanisms.

4.3. Can the EPS-membranes be applied for separation of sodium and potassium in practice?

Separation of two monovalent cations is a serious challenge,

even for the most advanced electro-membrane processes, such as electrodialysis. This is because these ions possess similar physicochemical properties, e.g., hydrated size. Most state-of-the-art ion exchange membranes lack selectivity for one specific ion (Luo et al., 2018). With the mimicked "bio-membranes" (ALG and EPS-membranes) as prepared in this study, a relatively high selectivity towards potassium over sodium ($S_{K^+/Na^+} > 1$) was observed, particularly for the ALG-membrane. Such selectivity was absent in a commercial cation-exchange membrane (Fig. 6-IV). However, the membranes prepared in this study cannot be considered for commercial application at this stage due to their limited stability. Approximately 48 h exposure of membranes to water leads to visible EPS detachment from the PVDF EPS-membrane and to water leakage in the ALG-membrane (data not shown). In the EPS-membrane, this is likely due to weak adhesion between EPS (hydrophilic with hydrophobic moieties) and PVDF (hydrophobic), whereas in the ALG-membrane this is likely due to Ca^{2+} exchange with Na^+, leading to disintegration of 3D structure of the gel (Lee and Mooney, 2012). Future studies need to focus on the EPS and sodium alginate properties that dictate the selective transport of K^+ over Na^+, which may help to develop analogous synthetic membranes. Such investigations should include fractionation of EPS extracts in their constituents and also preparation of membranes with EPS model constituents other than alginate (e.g., proteins and glycoproteins) to elucidate how these affect the membrane transport properties.

5. Concluding remarks and outlook

To date, only few studies have focused on transport of cations and anions through EPS layers of microbial biofilms, probably due to a lack of relatively simple methods. In this study, an electrochemical method with use of EPS-based membranes was shown to be effective in characterizing selectivity of EPS towards transport of monovalent ions. An unexpected result of this study was the selective transport of K^+ over Na^+ through EPS layers in an electrochemical cell. Despite the fact that the membranes as prepared in this study are of insufficient stability for commercial applications, the underlying mechanism for such selectivity should still be further investigated. A mechanistic understanding of K^+ selectivity in EPS layers could potentially lead to development of commercial membranes to treat e.g., green house water. Finally, while in literature EPS are sometimes mentioned as a potential protective barrier for microorganisms against high salinity, mechanistic explanations on how exactly EPS would be protective are scarcely reported. The cation exchange nature of EPS together with the ionic composition measurements of granular sludge, in which considerably smaller amounts of Cl^- were measured compared to the bulk liquid, suggest that EPS of the granules function as a protective barrier against anions. In addition, the cation interaction with the negatively charged functional groups of EPS could further alleviate salt toxicity by lowering the osmotic pressure "sensed" by the microorganisms. The suggested mechanism should be further explored.

Declaration of competing interest

The authors declare that they have no known competing financial interests or personal relationships that could have appeared to influence the work reported in this paper.

Appendix A. Supplementary data

Supplementary data to this article can be found online at https://doi.org/10.1016/j.watres.2020.115855.

References

Ahmed, E.M., 2015. Hydrogel: preparation, characterization, and applications: a review. J. Adv. Res. 6 (2), 105–121. https://doi.org/10.1016/j.jare.2013.07.006.

Ajao, V., Bruning, H., Rijnaarts, H., Temmink, H., 2018. Natural flocculants from fresh and saline wastewater: comparative properties and flocculation performances. Chem. Eng. J. 349, 622–632. https://doi.org/10.1016/j.cej.2018.05.123.

Altaş, L., 2009. Inhibitory effect of heavy metals on methane-producing anaerobic granular sludge. J. Hazard Mater. 162 (2), 1551–1556. https://doi.org/10.1016/j.jhazmat.2008.06.048.

Bell Jr., P.B., Lindroth, M., Fredriksson, B.-A., 1987. Use of sputter coating to prepare whole mounts of cytoskeletons for transmission and high-resolution scanning and scanning transmission electron microscopy. J. Electron. Microsc. Tech. 7 (3), 149–159. https://doi.org/10.1002/jemt.1060070302.

Chen, J.L., Ortiz, R., Steele, T.W.J., Stuckey, D.C., 2014. Toxicants inhibiting anaerobic digestion: a review. Biotechnol. Adv. 32 (8), 1523–1534. https://doi.org/10.1016/j.biotechadv.2014.10.005.

Chen, Y., Cheng, J.J., 2007. Effect of potassium inhibition on the thermophilic anaerobic digestion of swine waste. Water Environ. Res. 79 (6), 667–674. https://doi.org/10.2175/106143007x156853.

Comte, S., Guibaud, G., Baudu, M., 2006a. Relations between extraction protocols for activated sludge extracellular polymeric substances (EPS) and complexation properties of Pb and Cd with EPS: Part II. Consequences of EPS extraction methods on Pb2+ and Cd2+ complexation. Enzym. Microb. Technol. 38 (1–2), 246–252. https://doi.org/10.1016/j.enzmictec.2005.06.023.

Comte, S., Guibaud, G., Baudu, M., 2006b. Biosorption properties of extracellular polymeric substances (EPS) resulting from activated sludge according to their type: soluble or bound. Process Biochem. 41 (4), 815–823. https://doi.org/10.1016/j.procbio.2005.10.014.

Comte, S., Guibaud, G., Baudu, M., 2008. Biosorption properties of extracellular polymeric substances (EPS) towards Cd, Cu and Pb for different pH values. J. Hazard. Mater. 151 (1), 185–193. https://doi.org/10.1016/j.jhazmat.2007.05.070.

d'Abzac, P., Bordas, F., van Hullebusch, E., Lens, P.N.L., Guibaud, G., 2010. Effects of extraction procedures on metal binding properties of extracellular polymeric substances (EPS) from anaerobic granular sludges. Colloids Surf. B Biointerfaces 80 (2), 161–168. https://doi.org/10.1016/j.colsurfb.2005.043.

d'Abzac, P., Bordas, F., Joussein, E., van Hullebusch, E.D., Lens, P.N.L., Guibaud, G., 2013. Metal binding properties of extracellular polymeric substances extracted from anaerobic granular sludges. Environ. Sci. Pollut. Control Ser. 20 (7), 4509–4519. https://doi.org/10.1007/s11356-012-1401-3.

De Vrieze, J., Coma, M., Debeuckelaere, M., Van der Meeren, P., Rabaey, K., 2016. High salinity in molasses wastewaters shifts anaerobic digestion to carboxylate production. Water Res. 98, 293–301. https://doi.org/10.1016/j.watres.2016.04.035.

Dobrowolski, R., Szcześ, A., Czemierska, M., Jarosz-Wikołazka, A., 2017. Studies of cadmium(II), lead(II), nickel(II), cobalt(II) and chromium(VI) sorption on extracellular polymeric substances produced by Rhodococcus opacus and Rhodococcus rhodochrous. Bioresour. Technol. 225, 113–120. https://doi.org/10.1016/j.biortech.2016.11.040.

Echlin, P., 2009. Handbook of Sample Preparation for Scanning Electron Microscopy and X-Ray Microanalysis. Springer Science & Business Media, New York, USA. https://doi.org/10.1007/978-0-387-85731-2.

Epsztein, R., Shaulsky, E., Qin, M., Elimelech, M., 2019. Activation behavior for ion permeation in ion-exchange membranes: role of ion dehydration in selective transport. J. Membr. Sci. 580, 316–326. https://doi.org/10.1016/j.memsci.2019.02.009.

Fang, C., Boe, K., Angelidaki, I., 2011. Anaerobic co-digestion of desugared molasses with cow manure; focusing on sodium and potassium inhibition. Bioresour. Technol. 102 (2), 1005–1011. https://doi.org/10.1016/j.biortech.2010.09.077.

Felz, S., Al-Zuhairy, S., Aarstad, O.A., van Loosdrecht, M.C.M., Lin, Y.M., 2016. Extraction of structural extracellular polymeric substances from aerobic granular sludge. JoVE : JoVE (115), 54534. https://doi.org/10.3791/54534.

Flemming, H.-C., Wingender, J., 2010. The biofilm matrix. Nat. Rev. Microbiol. 8 (9), 623–633.

Gagliano, M., Ismail, S., Stams, A., Plugge, C., Temmink, H., Van Lier, J., 2017. Biofilm formation and granule properties in anaerobic digestion at high salinity. Water Res. 121, 61–71. https://doi.org/10.1016/j.watres.2017.05.016.

Gagliano, M.C., Neu, T.R., Kuhlicke, U., Sudmalis, D., Temmink, H., Plugge, C.M., 2018. EPS glycoconjugate profiles shift as adaptive response in anaerobic microbial granulation at high salinity. Front. Microbiol. 9, 1423. https://doi.org/10.3389/fmicb.2018.01423.

Galama, A.H., Post, J.W., Cohen Stuart, M.A., Biesheuvel, P.M., 2013. Validity of the Boltzmann equation to describe Donnan equilibrium at the membrane–solution interface. J. Membr. Sci. 442, 131–139. https://doi.org/10.1016/j.memsci.2013.04.022.

Geise, G.M., Hickner, M.A., Logan, B.E., 2013. Ionic resistance and permselectivity tradeoffs in anion exchange membranes. ACS Appl. Mater. Interfaces 5 (20), 10294–10301. https://doi.org/10.1021/am403207w.

Gutierrez, T., Shimmield, T., Haidon, C., Black, K., Green, D.H., 2008. Emulsifying and metal ion binding activity of a glycoprotein exopolymer produced by Pseudoalteromonas sp. strain TG12. Appl. Environ. Microbiol. 74 (15), 4867. https://doi.org/10.1128/aem.00316-08.

Gutierrez, T., Biller, D.V., Shimmield, T., Green, D.H., 2012. Metal binding properties of the EPS produced by Halomonas sp. TG39 and its potential in enhancing trace element bioavailability to eukaryotic phytoplankton. Biometals 25 (6), 1185–1194. https://doi.org/10.1007/s10534-012-9581-3.

Harrison, J.J., Ceri, H., Turner, R.J., 2007. Multimetal resistance and tolerance in microbial biofilms. Nat. Rev. Microbiol. 5, 928.

Horn, H., Morgenroth, E., 2006. Transport of oxygen, sodium chloride, and sodium nitrate in biofilms. Chem. Eng. Sci. 61 (5), 1347–1356. https://doi.org/10.1016/j.ces.2005.08.027.

Hosseini, S.M., Gholami, A., Madaeni, S.S., Moghadassi, A.R., Hamidi, A.R., 2012. Fabrication of (polyvinyl chloride/cellulose acetate) electrodialysis heterogeneous cation exchange membrane: characterization and performance in desalination process. Desalination 306, 51–59. https://doi.org/10.1016/j.desal.2012.07.028.

Hu, Z., Jin, J., Abruña, H.D., Houston, P.L., Hay, A.G., Ghiorse, W.C., Shuler, M.L., Hidalgo, G., Lion, L.W., 2007. Spatial distributions of copper in microbial biofilms by scanning electrochemical microscopy. Environ. Sci. Technol. 41 (3), 936–941. https://doi.org/10.1021/es061293k.

Ismail, S., de La Parra, C., Temmink, H., Van Lier, J., 2010. Extracellular polymeric substances (EPS) in upflow anaerobic sludge blanket (UASB) reactors operated under high salinity conditions. Water Res. 44 (6), 1909–1917. https://doi.org/10.1016/j.watres.2009.11.039.

Karri, S., Sierra-Alvarez, R., Field, J.A., 2006. Toxicity of copper to acetoclastic and hydrogenotrophic activities of methanogens and sulfate reducers in anaerobic sludge. Chemosphere 62 (1), 121–127. https://doi.org/10.1016/j.chemosphere.2005.04.016.

Körstgens, V., Flemming, H., Wingender, J., Borchard, W., 2001. Influence of calcium ions on the mechanical properties of a model biofilmof mucoid Pseudomonas aeruginosa. Water Sci. Technol. 43 (6), 49–57.

Kugelman, I.J., McCarty, P.L., 1965. Cation toxicity and stimulation in anaerobic waste treatment. Journal (Water Pollution Control Federation) 37 (1), 97–116.

Lee, K.Y., Mooney, D.J., 2012. Alginate: properties and biomedical applications. Prog. Polym. Sci. 37 (1), 106–126. https://doi.org/10.1016/j.progpolymsci.2011.06.003.

Lefebvre, O., Quentin, S., Torrijos, M., Godon, J.J., Delgenes, J.P., Moletta, R., 2007. Impact of increasing NaCl concentrations on the performance and community composition of two anaerobic reactors. Appl. Microbiol. Biotechnol. 75 https://doi.org/10.1007/s00253-006-0799-2.

Li, J., He, J., Huang, Y., Li, D., Chen, X., 2015. Improving surface and mechanical properties of alginate films by using ethanol as a co-solvent during external gelation. Carbohydr. Polym. 123, 208–216. https://doi.org/10.1016/j.carbpol.2015.01.040.

Li, W.-W., Yu, H.-Q., 2014. Insight into the roles of microbial extracellular polymer substances in metal biosorption. Bioresour. Technol. 160, 15–23. https://doi.org/10.1016/j.biortech.2013.11.074.

Lin, C.-Y., Chen, C.-C., 1999. Effect of heavy metals on the methanogenic UASB granule. Water Res. 33 (2), 409–416. https://doi.org/10.1016/S0043-1354(98)00211-5.

Lin, Y., Zhang, H., Adin, A., 2009. Characterization of bacterial alginate extracted from biofilm matrix. Desalination and Water Treatment 8 (1–3), 250–255. https://doi.org/10.5004/dwt.2009.791.

Lin, Y., de Kreuk, M., van Loosdrecht, M.C.M., Adin, A., 2010. Characterization of alginate-like exopolysaccharides isolated from aerobic granular sludge in pilot-plant. Water Res. 44 (11), 3355–3364. https://doi.org/10.1016/j.watres.2010.03.019.

Liu, Y., Fang, H.H.P., 2003. Influences of extracellular polymeric substances (EPS) on flocculation, settling, and dewatering of activated sludge. Crit. Rev. Environ. Sci. Technol. 33 (3), 237–273. https://doi-org.ezproxy.library.wur.nl/10.1080/10643380390814479.

Luo, T., Abdu, S., Wessling, M., 2018. Selectivity of ion exchange membranes: a

review. J. Membr. Sci. 555, 429–454. https://doi.org/10.1016/j.memsci.2018.03.051.

Martin, D.D., Ciulla, R.A., Roberts, M.F., 1999. Osmoadaptation in archaea. Appl. Environ. Microbiol. 65 (5), 1815–1825.

Martin, D.D., Ciulla, R.A., Robinson, P.M., Roberts, M.F., 2000. Switching osmolyte strategies: response of Methanococcus thermolithotrophicus to changes in external NaCl. Biochim. Biophys. Acta Gen. Subj. 1524 (1), 1–10. https://doi.org/10.1016/S0304-4165(00)00131-8.

McCarty, P.L., McKinney, R.E., 1961. Salt toxicity in anaerobic digestion. Journal (Water Pollution Control Federation) 33 (4), 399–415.

Mubita, T., Porada, S., Aerts, P., van der Wal, A., 2020. Heterogeneous anion exchange membranes with nitrate selectivity and low electrical resistance. J. Membr. Sci. https://doi.org/10.1016/j.memsci.2020.118000, 118000.

Nestle, N., Kimmich, R., 1996. Heavy metal uptake of alginate gels studied by NMR microscopy. Colloid. Surface. Physicochem. Eng. Aspect. 115, 141–147. https://doi.org/10.1016/0927-7757(96)03608-4.

Nightingale, E.R., 1959. Phenomenological theory of ion solvation. Effective radii of hydrated ions. J. Phys. Chem. 63 (9), 1381–1387, 10.1021/j150579a011.

Rinzema, A., van Lier, J., Lettinga, G., 1988. Sodium inhibition of acetoclastic methanogens in granular sludge from a UASB reactor. Enzym. Microb. Technol. 10 (1), 24–32. https://doi.org/10.1016/0141-0229(88)90094-4.

Roberts, M.F., 2005. Organic compatible solutes of halotolerant and halophilic microorganisms. Saline Syst. 1 (1), 5. https://doi.org/10.1186/1746-1448-1-5.

Sadrzadeh, M., Mohammadi, T., 2009. Treatment of sea water using electrodialysis: current efficiency evaluation. Desalination 249 (1), 279–285. https://doi.org/10.1016/j.desal.2008.10.029.

Seviour, T., Yuan, Z., van Loosdrecht, M.C., Lin, Y., 2012. Aerobic sludge granulation: a tale of two polysaccharides? Water Res. 46 (15), 4803–4813.

Seviour, T., Derlon, N., Dueholm, M.S., Flemming, H.-C., Girbal-Neuhauser, E., Horn, H., Kjelleberg, S., van Loosdrecht, M.C.M., Lotti, T., Malpei, M.F., Nerenberg, R., Neu, T.R., Paul, E., Yu, H., Lin, Y., 2019. Extracellular polymeric substances of biofilms: suffering from an identity crisis. Water Res. 151, 1–7. https://doi.org/10.1016/j.watres.2018.11.020.

Siegrist, H., Gujer, W., 1985. Mass transfer mechanisms in a heterotrophic biofilm. Water Res. 19 (11), 1369–1378. https://doi.org/10.1016/0043-1354(85)90303-3.

Smith, W.R., Moučka, F., Nezbeda, I., 2016. Osmotic pressure of aqueous electrolyte solutions via molecular simulations of chemical potentials: application to NaCl. Fluid Phase Equil. 407, 76–83. https://doi.org/10.1016/j.fluid.2015.05.012.

Sowers, K.R., Gunsalus, R.P., 1995. Halotolerance in methanosarcina spp.: role of N (sup (epsilon))-Acetyl-(beta)-Lysine,(alpha)-Glutamate, Glycine betaine, and K (sup+) as compatible solutes for osmotic adaptation. Appl. Environ. Microbiol. 61 (12), 4382–4388. https://www.ncbi.nlm.nih.gov/pubmed/16535193.

Steinbusch, K.J.J., Hamelers, H.V.M., Buisman, C.J.N., 2008. Alcohol production through volatile fatty acids reduction with hydrogen as electron donor by mixed cultures. Water Res. 42 (15), 4059–4066. https://doi.org/10.1016/j.watres.2008.05.032.

Sudmalis, D., Gagliano, M.C., Pei, R., Grolle, K., Plugge, C.M., Rijnaarts, H.H.M., Zeeman, G., Temmink, H., 2018a. Fast anaerobic sludge granulation at elevated salinity. Water Res. 128 (Suppl. C), 293–303. https://doi.org/10.1016/j.watres.2017.10.038.

Sudmalis, D., Millah, S.K., Gagliano, M.C., Butré, C.I., Plugge, C.M., Rijnaarts, H.H.M., Zeeman, G., Temmink, H., 2018b. The potential of osmolytes and their precursors to alleviate osmotic stress of anaerobic granular sludge. Water Res. 147, 142–151. https://doi.org/10.1016/j.watres.2018.09.059.

Suzuki, I., Lee, D., Mackay, B., Harahuc, L., Oh, J.K., 1999. Effect of various ions, pH, and osmotic pressure on oxidation of elemental sulfur by thiobacillus thiooxidans. Appl. Environ. Microbiol. 65 (11), 5163.

Teitzel, G.M., Parsek, M.R., 2003. Heavy metal resistance of biofilm and planktonic Pseudomonas aeruginosa. Appl. Environ. Microbiol. 69 (4), 2313. https://doi.org/10.1128/aem.69.4.2313-2320.2003.

Toner, B., Manceau, A., Marcus, M.A., Millet, D.B., Sposito, G., 2005. Zinc sorption by a bacterial biofilm. Environ. Sci. Technol. 39 (21), 8288–8294. https://doi.org/10.1021/es050528+.

Vyrides, I., Stuckey, D., 2009. Adaptation of anaerobic biomass to saline conditions: role of compatible solutes and extracellular polysaccharides. Enzym. Microb. Technol. 44 (1), 46–51. https://doi.org/10.1016/j.enzmictec.2008.09.008.

Vyrides, I., Santos, H., Mingote, A., Ray, M., Stuckey, D., 2010. Are compatible solutes compatible with biological treatment of saline wastewater? Batch and continuous studies using submerged anaerobic membrane bioreactors (SAMBRs). Environ. Sci. Technol. 44 (19), 7437–7442. https://doi.org/10.1021/es903981k.

Wang, H., Wilksch, J.J., Lithgow, T., Strugnell, R.A., Gee, M.L., 2013. Nanomechanics measurements of live bacteria reveal a mechanism for bacterial cell protection: the polysaccharide capsule in Klebsiella is a responsive polymer hydrogel that adapts to osmotic stress. Soft Matter 9 (31), 7560–7567. https://doi.org/10.1039/c3sm51325d.

Welte, C., Deppenmeier, U., 2014. Bioenergetics and anaerobic respiratory chains of aceticlastic methanogens. Biochim. Biophys. Acta Bioenerg. 1837 (7), 1130–1147. https://doi.org/10.1016/j.bbabio.2013.12.002.

Zhou, W., Imai, T., Ukita, M., Sekine, M., Higuchi, T., 2006. Triggering forces for anaerobic granulation in UASB reactors. Process Biochem. 41 (1), 36–43. https://doi.org/10.1016/j.procbio.2005.02.029.